ACS APPLIED MATERIALS & INTERFACES

Research Article

Cite This: ACS Appl. Mater. Interfaces 2018, 10, 4173−4182

www.acsami.org

Marine Antifouling Behavior of Lubricant-Infused Nanowrinkled Polymeric Surfaces

Cameron S. Ware,[†] Truis Smith-Palmer,[‡] Sam Peppou-Chapman,[†] Liam R. J. Scarratt,[†] Erin M. Humphries,[†] Daniel Balzer,[†] and Chiara Neto*[,†]

[†]School of Chemistry and University of Sydney Nano Institute, The University of Sydney, NSW 2006, Australia

[‡]Department of Chemistry, St. Francis Xavier University, 2321 Notre Dame Avenue, Antigonish, Nova Scotia B2G 2W5, Canada

Supporting Information

ABSTRACT: A new family of polymeric, lubricant-infused, nanostructured wrinkled surfaces was designed that effectively retains inert nontoxic silicone oil, after draining by spin-coating and vigorous shear for 2 weeks. The wrinkled surfaces were fabricated using three different polymers (Teflon AF, polystyrene, and poly(4-vinylpyridine)) and two shrinkable substrates (Polyshrink and shrinkwrap), and Teflon on Polyshrink was found to be the most effective system. The volume of trapped lubricant was quantified by adding Nile red to the silicone oil before infusion and then extracting the oil and Nile red from the surfaces in heptane and measuring by fluorimetry. Higher volumes of lubricant induced lower roll-off angles for water droplets, and in turn induced better antifouling performance. The infused surfaces displayed stability in seawater and inhibited growth of *Pseudoalteromonas spp*. bacteria up to 99%, with as little as 0.9 μL cm^{-2} of the silicone oil infused. Field tests in the waters of Sydney Harbor over 7 weeks showed that silicone oil infusion inhibited the attachment of algae, but the algal attachment increased as the silicone oil was slowly depleted over time. The infused wrinkled surfaces have high transparency and are moldable, making them suited to protect the windows of underwater sensors and cameras.

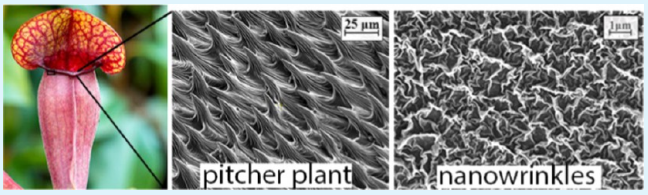

KEYWORDS: *marine fouling, liquid-infused surfaces, surface wettability, nanostructured surfaces, SLIPS, biofouling, structured surfaces*

INTRODUCTION

The ecological and economic impact of marine fouling is devastating, affecting wild fisheries, aquaculture, marine sensors, shipping, and corrosion.[1] The adverse effects include increased drag on ship hulls, spread of invasive species, damage to aquaculture (estimated cost U.S. $1.5−3 billion/year),[2] and threats to public health due to toxic algae and bacteria. Marine biofouling involves several steps: initial conditioning by adsorption, bacterial attachment, formation of a surface biofilm, and attachment of larger marine organisms, such as barnacles and algae. A number of strategies to fabricate antifouling coatings that resist adhesion of biocontaminants, or degrade or kill them, have been developed (see recent review[3]). The methods include using polymers based on poly(dimethylsiloxane) (PDMS), using specific topography, or releasing biocides. The use of tributyl tin, a successful antifouling agent, has been banned in most countries due to its toxic effect on marine life, renewing the need for nontoxic approaches. Among the most recent approaches are slippery porous lubricant-infused surfaces (SLIPS), which mimic the pitcher plant and are developed by the Aizenberg group.[4−6] These surfaces resist biofouling by trapping a lubricant layer by the capillary forces within a surface micro- and nanostructure. The range of size and spacing of the features that are effective at trapping a given lubricant depends on the interfacial tensions of the solid surface/lubricant/working liquid system under study, and many examples exist in the literature (see recent review[7] on fabrication approaches, including transparent platforms[8,9]). However, the stability of the lubricating film, crucial to the function of the surfaces, is under intense scrutiny. Evidence suggests that it can be depleted by exposure to a high shear, causing the loss of anti-adhesive properties.[10−12] A complete understanding of the most efficient structures for lubricant retention under flow does not exist.[10] In addition, the minimum thickness of lubricant needed or the effectiveness of a partly filled structure in preventing adhesion is not known. A thorough understanding of the amount of liquid infused and its stability under shear will facilitate the implementation of antifouling SLIPS.

Methods to estimate film thickness have relied on mass change, limiting their effectiveness to thick oil layers.[9,13] Only recently, the film thickness of oil has been estimated to a higher precision on a permeable membrane using porometry,[14] and on transparent surfaces using thin-film interference.[15] However, neither of these methods can quantify the amount of oil on nontransparent or nonpermeable surfaces, which are very commonly used surfaces in the literature.

Here, we mimic the lubricating mechanism of the pitcher plant using nanostructured wrinkled polymer surfaces. Our wrinkle

Received: October 5, 2017
Accepted: December 18, 2017
Published: December 18, 2017

DOI: 10.1021/acsami.7b14736
ACS Appl. Mater. Interfaces 2018, 10, 4173−4182

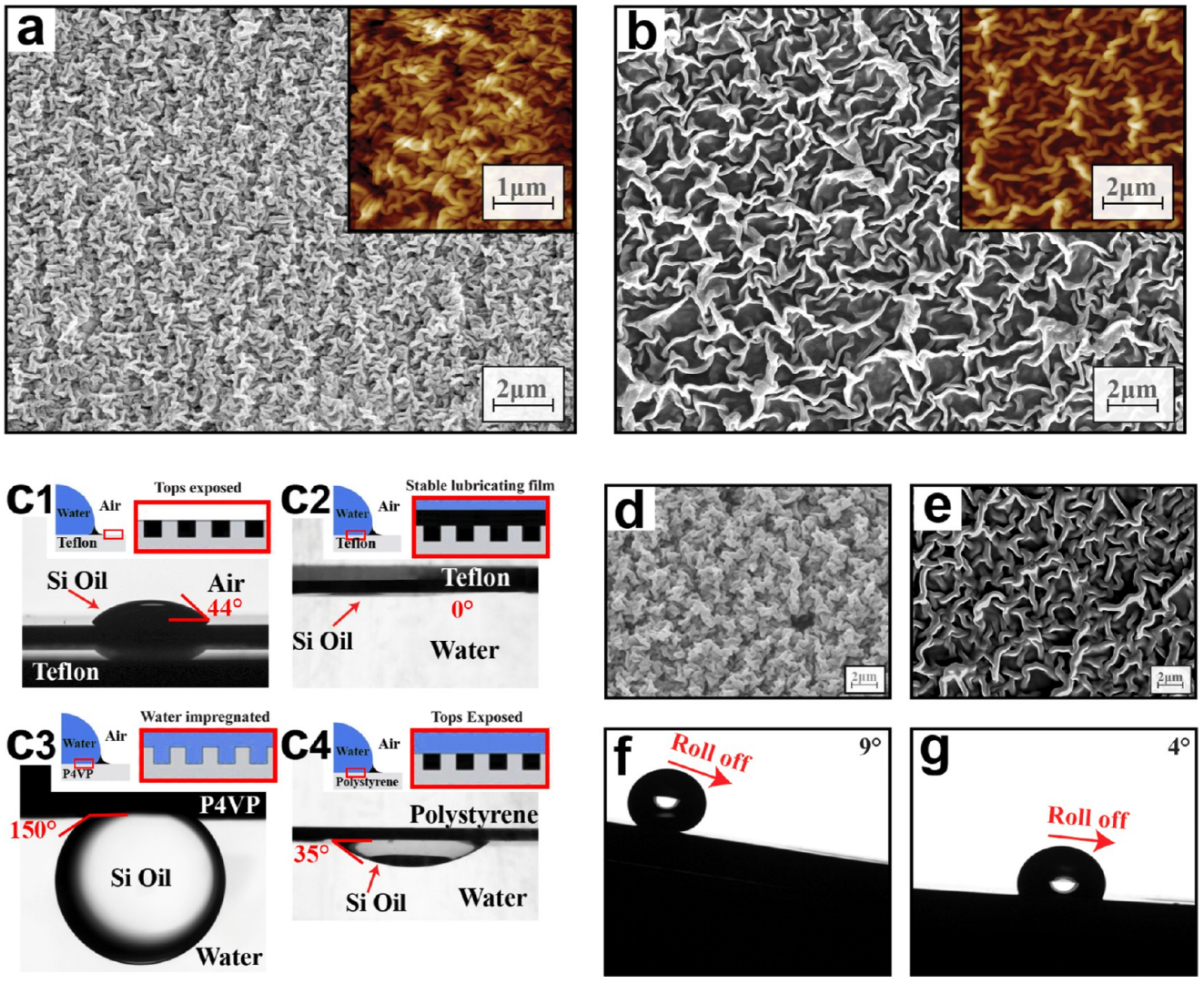

Figure 1. SEM micrograph of (a) Teflon wrinkles on Polyshrink, λ = 147 nm; inset: AFM micrograph, height scale 800 nm; and (b) Teflon wrinkles on shrinkwrap, λ = 390 nm, AFM height scale 1 μm. (c) Micrographs of silicone oil droplets on (c1) flat Teflon in air, (c2) under water, (c3) on wrinkled P4VP, and (c4) PS in water; insets show the thermodynamically stable configuration for the corresponding infused wrinkled interface, with silicone oil (black) and water (blue). (d) P4VP wrinkles on Polyshrink with λ = 370 nm and (e) PS wrinkles on shrinkwrap wrinkles with λ = 800 nm. Water droplets rolling off (f) dry and (g) infused Teflon wrinkles, λ = 147 nm.

system is shown to trap a lubricant as the pitcher plant structure traps water, but our topography is on a much smaller length scale than in the plant. The wrinkled surfaces are shown to be slippery (i.e., they shed water droplets readily) and inhibit the attachment of bacteria and algae under water. The performance of these surfaces was tested through field tests in a marine environment. For the first time in the literature on SLIPS, the amount of lubricant on the surface was quantified on a nonporous, structured, solid substrate using a fluorescence protocol, and related to its antifouling performance. As little as 0.04 μL cm^{-2} of lubricant, which was retained after 2 weeks of vigorous shear, was found to inhibit bacterial fouling. A detailed comparison with published papers is included, and our surfaces are found to be competitive with existing SLIPS. To our knowledge, bacterial attachment has not been tested before on surfaces aged using underwater shear, which is a key aspect to moving toward their successful application. The real-world antifouling performance was tested through a field test in Sydney Harbor, showing that the infused surfaces are fouled much less than their uninfused counterparts. Only one other study has examined the efficacy of SLIPS in a field setting[16] by testing the attachment of mussels and other fouling species on infused PDMS substrates. Our wrinkle fabrication approach compares favorably with the existing approaches using lithography,[17−19] electrodeposition,[20] and sol−gel processes.[21] Our nanoscale wrinkles are spontaneously formed, very easy to produce and tune, and robust to wear and scratches,[22] which give them real potential for use in screening studies for different lubricants and material properties. Compared to other self-assembled polymer surfaces,[23,24] they have the advantage of being effective for long periods of time in the high ionic strength of seawater, where many soft polymeric coatings delaminate. In addition, they can be made highly transparent and molded to shape, giving them a wide applicability.

MATERIALS AND METHODS

Wrinkle Preparation and Characterization. Teflon AF 1600 (DuPont), polystyrene (PS, Polymer Standards Service, MW = 96 000), or poly(4-vinylpyridine) (P4VP, Aldrich, MW = 60 000) were spin-coated (Laurell Technologies) onto Polyshrink or shrinkwrap (Get Packed Packing, identified as polyethylene, Figure S1).

DOI: 10.1021/acsami.7b14736
ACS Appl. Mater. Interfaces 2018, 10, 4173−4182

Table 1. Wrinkle Wavelength and Wettability Data for Wrinkled Polymer Surfaces before (Dry) and after Infusion (Infused) with Silicone Oil 10 cSt[a]

substrate	top film thickness, nm	wrinkle wavelength, nm	wrinkle height, nm	dry		infused	
				static water contact angle, deg	water roll-off angle, deg	static water contact angle, deg	water roll-off angle, deg
Top Film Teflon							
silicon wafer	100	flat	flat	121 ± 1	22 ± 1	N/A	N/A
Polyshrink	13	90 ± 10	130 ± 7	166 ± 3	12 ± 1	114 ± 1	4 ± 1[b]
	34	150 ± 20	290 ± 30	168 ± 2	9 ± 1	115 ± 1	4 ± 1[b]
	168	1190 ± 100	1100 ± 80	160 ± 4	17 ± 6	117 ± 1	9 ± 1
shrinkwrap[d]	20	150 ± 20	180 ± 50	163 ± 4	10 ± 6	106 ± 1	3 ± 1[b]
	60	390 ± 70	380 ± 90	166 ± 5	10 ± 3	113 ± 1	4 ± 1[b]
Top Film PS							
silicon wafer	100	flat	flat	92	30	N/A	N/A
shrinkwrap[d]	68	480 ± 70	300 ± 100	100	>180	N/A[c]	<5[c]
	95	800 ± 200	600 ± 300	116	>180	N/A[c]	<5[c]

[a]Mean value and standard deviation shown. [b]These values remained unaltered after 7 days. [c]Water droplets rolled off the surface before the CA could be measured. [d]Degree of shrinking was to 15% of original surface area.

Shrinkwrap was preshrunk onto glass slides before spin-coating. Film thickness was quantified by ellipsometry (J.A. Woollam, M2000). Shrinking was performed at 160 °C, 2 min for Teflon/Polyshrink, at 130 °C for P4VP/Polyshrink, and at 110 °C for shrinkwrap. Topography was characterized with a scanning electron microscope (Zeiss EVO/Qemscan) and an atomic force microscope (Bruker Multimode 8). Static contact angle and roll-off angle of water (KSV Cam 200) were measured at various stages before and after infusion. Transparent substrates were prepared using the transparent variety of Polyshrink. Curved surfaces were prepared by molding the malleable substrate while it was still hot.

Wrinkle Infusion. Infusion of silicone oil (Sigma-Aldrich, 10 cSt, density 0.93 g mL^{-1}) into wrinkles was performed using a KSV NIMA dip coater, or manually by spreading 10 μL over the surface for 24 h. The latter initially gave a surface with a large excess of oil. Drained wrinkles could be obtained by withdrawing surfaces from oil at a slow rate (0.2 mm min^{-1}),[25] draining surfaces vertically for 1 h or more, or spinning excess oil off for 1−5 min at 8000 rpm in a spin-coater.

Bacterial Attachment Tests. Surfaces were exposed to *Pseudoalteromonas spp.* (OD_{600nm} = 0.25) in tryptic soy broth/artificial seawater, 3:1[26] for 1 h, then shaken at 150 rpm in fresh medium for 24 h at ambient temperature on an orbital shaker (Ratek). Addition of aqueous crystal violet (0.1%, Sigma-Aldrich) turned the biofilm purple,[26] before extraction into 30% acetic acid to measure absorbance (590 nm).

Shear Test. Wrinkled Teflon surfaces (1 cm^2) were glued (Selleys AQUAFIX) to the inside lid of 20 mL vials of the artificial seawater and rotated (roller mixer, Ratek) at 60 rpm for 2 weeks before bacterial testing. The roller mixer simulates vigorous shear in the ocean, as it has an angular velocity (from spinning) and two linear velocity vectors (parallel and perpendicular to the surface). The maximum parallel velocity was estimated to be ∼9 cm s^{-1} and the maximum perpendicular velocity ∼2 m s^{-1}.

Fluorescence Protocol for Oil Quantification. A 1.0 μM stock solution of Nile red in silicone oil was prepared by adding 5.0 μL of 0.20 mM Nile red (Sigma) in ethanol to 1.0 mL 10 cSt silicone oil (Sigma-Aldrich) and then stirring until the ethanol had evaporated and the oil was pale yellow. The stock solution of Nile red was used to infuse surfaces when the amount of oil held by a surface was to be determined. For the extraction of the oil, surfaces (1 cm^2) infused with silicone oil containing 1.0 μM Nile red were immersed in 2.5 mL heptane and sonicated for 0.5 min. Fluorescence (525 nm) was measured on a Cary Eclipse fluorimeter (Agilent) (excitation 484 nm, 20 nm slits). The amount of oil was determined by comparison to a standard curve prepared by diluting the aliquots of 1.0 μM Nile red in silicone oil with *n*-heptane. The method was further validated by determining the recovery of Nile red after adding discrete aliquots to the test surfaces but not carrying out any treatments to remove any before the analysis (Table S3).

Transmittance Measurements. Model surfaces (2 cm × 1 cm) were submerged in MilliQ water in a cuvette and the transmittance measured using a Shimadzu UV-2450 UV−Visible Spectrophotometer in double-beam mode.

Marine Fouling Test. The marine fouling test was performed at Watsons Bay, NSW, Australia (33°50′37.7″S, 151°16′53.4″E). Wrinkled surfaces (5 cm × 2.5 cm) were prepared as mentioned above. Uninfused Teflon wrinkles were used as controls, whereas the test surfaces were Teflon wrinkles infused with silicone oil and drained vertically for 1 h. Two support Perspex plates (3 mm thick) were prepared: the first plate was a control, and seven uninfused wrinkled Teflon surfaces (entirely free of silicone oil) were attached on it (with marine epoxy, Selleys AQUAFIX). On the second Perspex support plate were attached seven control surfaces and seven test surfaces in an alternating pattern. The plates were attached to a shark net using zip ties. The test was run for a total of 7 weeks from June to August 2017. Although the test was run during the Australian winter, the water temperature never dropped below 19 °C during the test.

The surfaces were removed from the ocean and stored in seawater before the analysis. Each surface was photographed without any treatment and then after rinsing (vigorous washing under the laboratory tap), and the images analyzed using ImageJ and Photoshop. Photoshop was used to crop the images, remove any distortion, and flatten the lighting. The images were then converted to grayscale in ImageJ and a threshold applied to identify the % area that had been fouled. Significance was assessed using a two-way ANOVA.

RESULTS

Wrinkle Optimization. The wrinkled surfaces are prepared by applying a rigid polymer layer (Teflon, polystyrene (PS), or poly(4-vinylpyridine) (P4VP)) on top of shrinkable substrates through spin-coating. The substrates included sheet-extruded PS (Polyshrink), or polyethylene shrinkwrap, which shrink to about 20 or 15%, respectively, of their original size upon heating (Figure S2). This shrinking results in the wrinkling of the rigid top polymer film.[22] Figure 1a shows the micrographs of the Teflon wrinkles, and Table 1 summarizes their typical dimensions and wettability properties. Four polymer−substrate combinations were tested (and more than 14 wrinkle sizes): Teflon on Polyshrink and shrinkwrap, PS on shrinkwrap, and P4VP on Polyshrink. The optimal combination, in terms of wrinkle reproducibility and infusion with silicone oil, was Teflon on Polyshrink. The Teflon wrinkles on Polyshrink were single scale, with the wavelength (λ = 85−1200 nm) and height (130−1100 nm) increasing proportionally with the initial Teflon film thickness (Table 1), as expected.[22]

Teflon wrinkles on shrinkwrap could be produced with a single-scale (Table 1), or a hierarchical double-scale, roughness

DOI: 10.1021/acsami.7b14736
ACS Appl. Mater. Interfaces 2018, 10, 4173−4182

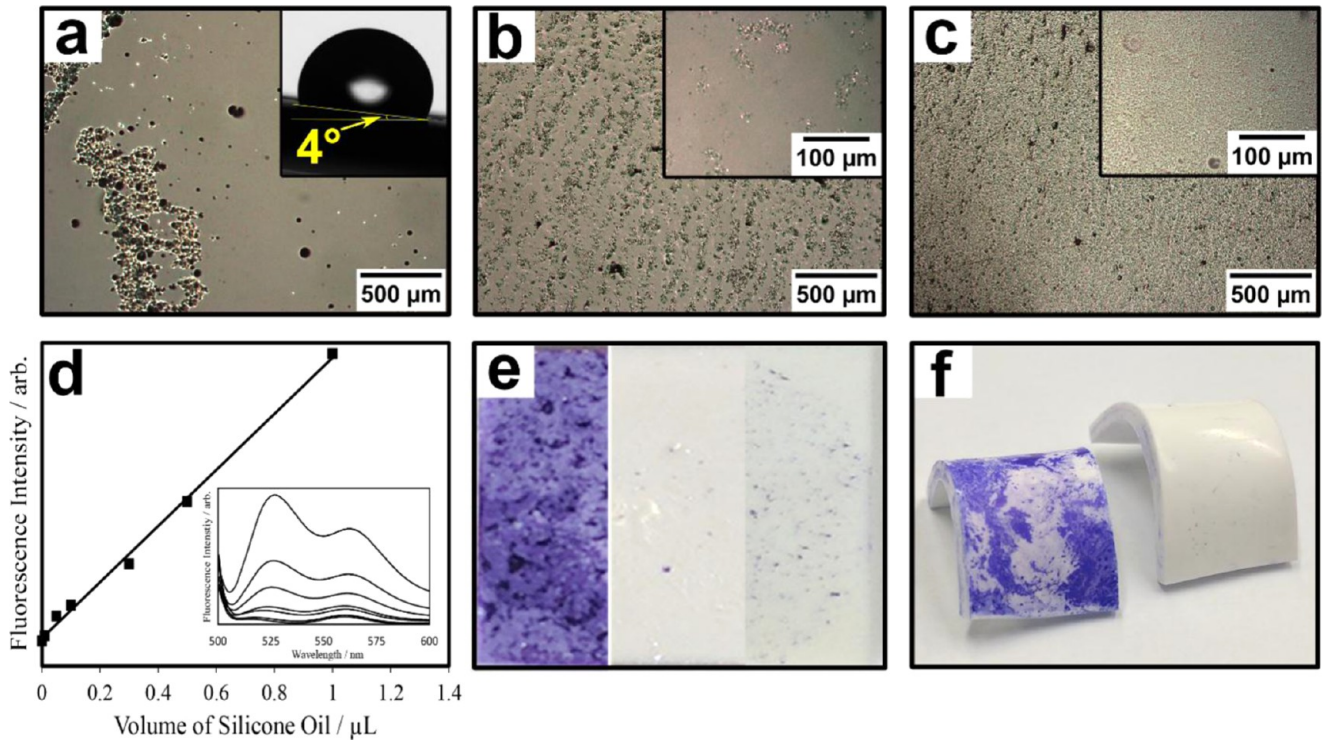

Figure 2. (a–c) Optical micrographs (OM) of wrinkled Teflon surfaces infused with silicone oil and drained for 1 h (a) or spun for 1 min (b) or 5 min (c) at 8000 rpm. Inset: (a) water drop rolling off surface at 4°; (b, c) higher magnifications of the OM; (d) calibration curve for Nile red in silicone oil in heptane. λ_{ex} = 484 nm, λ_{em} = 525 nm, 20 nm slits, inset: fluorescence emission spectra (λ_{ex} = 484 nm) for varying volumes (0–1.00 μL) of 1.00 μM Nile red in 10 cSt silicone oil; (e) samples stained with crystal violet after bacterial adhesion test with Psuedoalteromonas spp: dry Teflon wrinkles (left), infused Teflon wrinkles drained 1 h (center); infused Teflon wrinkles spun 1 min and exposed to vigorous shear in seawater for 2 weeks (right); (f) Teflon wrinkles were molded to a curved shape and exposed to bacteria: uninfused (left) and infused, drained 1 h (right).

(Figure S3, Table S1). Single-scale wrinkles are formed by limiting the degree of shrinking to 15% of the original surface area; allowing substrates to shrink further (to 10%) leads to nanoscale wrinkles on top of the microscale folds. The Teflon wrinkles are superhydrophobic (Table 1, contact angle >160°). The wettability of the dry Teflon wrinkles does not vary (not statistically different at the 95% confidence level) with the wrinkle size within the range tested. The roll-off angles (9–17°) are characteristic of a surface with a single-scale roughness, with water droplets in a partially collapsed Cassie–Baxter state.[27]

The wrinkled PS surfaces are single scale, but only hydrophobic, with water droplets pinning to the surface (Figure 1e and Table 1). P4VP wrinkles have a double-scale roughness and are hydrophilic (Figure 1d and Table S2).

Theory on Lubricant Infusion. The infusion of Teflon wrinkles with silicone oil results in a thermodynamically stable configuration, as established from the calculation of the critical contact angle for infusion (θ_c). When the contact angle of a liquid droplet on a flat surface is lower than θ_c, the droplet penetrates into the microstructure[25,28]

$$\cos\theta_c = \frac{1-\varphi}{r-\varphi}$$

where φ corresponds to the fraction of the solid surface wet by the liquid, and r is the roughness ratio. The φ factor for the wrinkles is estimated using the Cassie–Baxter equation[29]

$$\cos\theta^* = \varphi(\cos\theta + 1) - 1$$

where θ is the static water contact angle on a flat substrate (θ = 121° for Teflon) and θ^* is the static contact angle on the structured surface (θ^* = 164° for wrinkled Teflon).

The roughness ratio r is defined as the ratio of true surface area to apparent surface area. This ratio was approximated to the ratio of the original sample surface area to the final sample surface area after shrinking. Shrinkwrap and Polyshrink shrink to ~15 and ~20% of their original surface area, respectively, giving an estimated roughness ratio of 6.67 and 5, respectively. As both φ and r are estimates, only an approximation can be obtained for the critical contact angle, which is $\theta_c \approx 80°$ for wrinkles on both shrinkwrap and Polyshrink. For our system, the static contact angle of silicone oil on the flat Teflon surfaces in air is 44° (Figure 1c1) and completely spreads underwater (0° contact angle, Figure 1c2). In air, the silicone oil penetrates into the microstructure, as it is below the critical contact angle ($\theta_c \approx 80°$), and covers the structure fully underwater as it completely spreads underwater, producing a stable lubricant-infused coating in both scenarios.[25,28] A similar calculation gives $\theta_c \approx 86°$ and $\theta_c \approx 93°$ for PS and P4VP wrinkles, respectively; silicone oil is expected to infuse into the microstructure for both in air, but not underwater (data for flat surfaces not shown).

Infusion of Silicone Oil on the Wrinkled Surfaces. Silicone oil is applied onto the surfaces by spreading drops or by dip-coating. Excess oil is then drained by standing the surfaces vertically, spinning, or exposing to strong shear under water. The successful infusion of Teflon wrinkles on both Polyshrink and shrinkwrap is confirmed by the marked decrease in the roll-off angle of water droplets.[18] Surfaces with wrinkle λ between 85 and 390 nm display similar results, with the roll-off angles decreasing from a maximum of 12° (dry surface) to 4° (infused surface) (Figure 1f,g, Table 1). The roll-off angles on larger wrinkles (λ = 1190 nm) decrease from 17° (dry) to 9° (infused). These higher values are likely due to a larger fraction

DOI: 10.1021/acsami.7b14736
ACS Appl. Mater. Interfaces 2018, 10, 4173–4182

of the tops of the wrinkles being exposed to water. The lower infused roll-off angles for nanostructured surfaces, compared to microstructured surfaces, suggest that the former may perform better in antifouling applications. Roll-off angles of <1° were measured for infused surfaces with excess oil (Figure S4). However, this scenario is not sustainable, as the large wetting ridge formed around the water droplets (Figure S5) would gradually deplete the excess oil as the water droplets roll off the surface taking large volumes of oil with them. Teflon wrinkles obtained from the 34 nm thick Teflon layer are selected for further testing, as they have the minimum roll-off angle with minimum coating thickness, to give maximum cost-effectiveness.

Once infused in the surface, the lubricant affords the samples favorable properties associated with SLIPS.[18] The infused surfaces resist staining from water- and oil-based markers (Figure S6); (iii) silicon oil flows and fills in the scratches, self-healing any damage, such that the water droplets do not become pinned on the scratch as they would on a superhydrophobic surface (Figure S7).

Quantification of Silicone Oil in the Wrinkles. Optical microscopy (OM) of infused surfaces shows different amounts of oil on the surfaces, from none for dry wrinkles (featureless in OM), to pools of oil of various sizes, to a thick layer covering the whole structure when excess oil is present. The pools of oil decreases in size as the surfaces are drained vertically or spun at high rates (8000 rpm) for longer times (Figure 2a–c). As the draining progresses, more of the microstructure of the wrinkles becomes visible by OM.

The amount of silicone oil infused on the surfaces is quantified by a fluorescence method. Silicone oil containing 1.0 μM of Nile red is used to infuse the surfaces. After treatment (e.g., draining or submersing in seawater), the silicone oil and dye are extracted out of the wrinkles into *n*-heptane and the fluorescence of the resulting solution is measured. Heptane is chosen as a solvent because it is a good solvent for both Nile red and silicone oil and is nonvolatile and nonfluorescent. The amount of oil is determined by comparison to a standard curve prepared by diluting the aliquots of 1.0 μM Nile red in silicone oil with *n*-heptane. The emission spectra gives two peaks, one at 525 nm and another at 565 nm. The peak at 525 nm is selected for the calibration curve, as it is more sensitive, with a slope of 808 μL^{-1} as opposed to 565 μL^{-1} (Figure 2d). The standard curve is linear. The reproducibility varies from 0.1 to 4% (n = 5) as the aliquot size decreases from 1.0 to 0.050 μL. The recovery of the infused oil is 101 ± 13% (Table S3).

Surfaces with slippery properties, as revealed by the roll-off angles of ~5°, contain as little as 0.9 μL cm^{-2} of oil (Table 2). The amount of oil decreases to ~0.3 μL cm^{-2} by spinning the surfaces at 8000 rpm for 5 min, with a small increase in the roll-off angle (to 9°). Vigorous shear in seawater for 2 weeks reduces the amount of oil to 0.04 μL cm^{-2}, but the roll-off angle remains low (6–8°, Table 2).

The wrinkle structure optimized here retains the silicone oil well, as established on the basis of exposure to spinning and vigorous shear (see Table 3 below for a detailed comparison). It has been shown that random surface structures are advantageous in reducing the lubricant drainage, as compared to the regularly ordered structures.[30] The interwrinkle space might provide large oil reservoirs that disrupt the continuity of the infused lubricant, thereby preventing the liquid from draining, in a manner similar to the chemical patterning studied by the Stone group.[12] The reservoirs may replenish the surface over time and allow the surface to self-heal the scratches, as observed with microporous surfaces[18] (Figure S5).

Table 2. Quantification of Silicone Oil Content on Teflon Wrinkles of Wavelength λ =147 nm, Resulting Water Contact Angle and Roll-off Angles, and Bacterial Inhibition As Tested by Absorbance of Crystal Violet Extracted from the Surfaces Exposed to Bacteria

drainage treatment	volume silicone oil, μL cm^{-2}	water contact angle, deg	roll-off angle, deg	% inhibition[a]
drained 1 h	0.9 ± 0.2	99 ± 2	5 ± 1	99 ± 1
spun at 8000 rpm, 1 min	0.4 ± 0.2	111 ± 2	7 ± 1	86 ± 9
spun at 8000 rpm, 5 min	0.3 ± 0.2	113 ± 3	9 ± 1	84 ± 10
drained 1 h, 2 weeks shear	0.04 ± 0.01	113 ± 1	6 ± 3	73 ± 13
spun at 8000 rpm, 1 min, 2 weeks shear	0.02 ± 0.01	122 ± 6	8 ± 4	76 ± 16

[a]The % inhibition is relative to dry Teflon wrinkles, noninfused with silicone oil.

Only Teflon wrinkles are successfully infused with silicone oil under water (Figure 1c2). Silicone oil did not spread on a P4VP surface under water (contact angle 124–156°, Figure 1c3 and Table S2), with water preferentially wetting the surface due to its hydrophilicity (as confirmed by staining with aqueous crystal violet solution, Figure S8). Similarly, silicone oil did not spread on PS under water (contact angle 35°, Figure 1c4).[31] Because of this lack of a stable oil layer under water, neither P4VP nor PS wrinkles are tested for antifouling.

Inhibition of Marine Bacteria Attachment on Infused Wrinkled Surfaces. Superhydrophobic surfaces are known to be ineffective antibacterial coatings. The air layer trapped in the roughness underwater is metastable and collapses over time due to shear or pressure,[32] allowing a biofilm to form on the rough surface.[33] For our infused Teflon surfaces, the lubricant layer is thermodynamically stable, as shown above, preventing the collapse of water into the roughness.

To test antifouling properties, surfaces are exposed to marine bacteria, *Psuedoalteromonas spp*., for an hour, rinsed, and then immersed for 24 h in fresh seawater medium rich in nutrients. Application of crystal violet stain shows that a biofilm is readily formed on dry Teflon wrinkles (Figure 2e, left). The presence of infused silicone oil almost completely prevents the attachment of bacteria (Figure 2e(center and right),f). The extent of inhibition is 99 ± 1% for the infused Teflon surfaces drained for an hour, which holds ~0.9 μL cm^{-2} of silicone oil (Table 2). If the wrinkles are violently drained of oil by high rate spinning, or rotated in seawater for extended times (2 weeks), the extent of inhibition is only slightly reduced, to 84 ± 10 and 76 ± 16%, respectively. The inhibition potential of the surfaces correlates with lower water roll-off angles and larger pools of silicone oil. The silicone oil is not in itself toxic, as tested by studying bacterial growth in the presence of 1% silicone oil (Table S4). Bacterial attachment for several strains is known to be reduced on soft substrates,[34,35] and liquid silicone oil offers a soft and mobile layer on which contact points between the bacteria and the solid surface are reduced.[36]

Ability To Be Molded. An advantage of using polymer substrates is that they can be easily molded to a shape during fabrication. After the polystyrene substrate has been annealed, it is still malleable and able to be molded to a desired shape. An infused curved substrate is still very effective in resisting biofouling (Figure 2f), and before infusion remains superhydrophobic. Little change in the surface wrinkles is observed after molding (see Figure S9 for an example SEM from a curved

DOI: 10.1021/acsami.7b14736
ACS Appl. Mater. Interfaces 2018, 10, 4173–4182

Table 3. Comparison of Literature Results on Lubricant-Infused Surfaces[a]

	current study	Doll et al.[42]	Wei et al.[9]	Wang et al.[8]	Xiao et al.[44]	Zhang et al.[45]	Kovalenko et al.[37] and Amini et al.[16b]	Yuan et al.[43]	Yuan et al.[46]	Epstein et al.[4] and Wong et al.[18b]	Tesler et al.[47]
material and fabrication method	wrinkled Teflon	laser irradiated titanium	sol–gel coating	silanized roughened glass	polymer on glass	polymer coated glass	swollen PDMS	wrinkled SIBS	blow-spun SIBS microfiber	porous PTFE membrane	electrochemical TO on steel
surface structure	wrinkles	microspikes/-grooves	nanoscale roughness	nanosheets	network of polymer globules	network of microspheres	N/A	wrinkles	microfiber network	nanofiber network	microislands/nano-flakes
lubricant	silicone oil	PFPE	silicone oil	PFPE	PFPE	perfluorodeca-lin/PFPE	silicone oil	prefluordecalin	silicone oil/-PFPE	PFPE	PFPE
aging method	roller mixer (14 days, 60 rpm)	vertical storage (15 days), orbital shaker (5 h, 150 rpm)	centrifuge (1 min, 3500 rpm)	orbital shaker (20 days, 0.1–0.8 m s^{-1} flow), sonication	orbital shaker (28 days, 50 rpm)	N/A	N/A	N/A	N/A	N/A	N/A
lubricant quantification after aging	Y	N	Y	N/A	N/A	N/A	N/A	N/A	N/A	N/A	N/A
wettability	5 ± 1°[c]	<5°[d]	<5°[d]	< 5°[d]	~6°[d]	10°[c]	N/A	not measured	4.1 ± 0.9°[d]	5°[d]	1.4–3°[d]
wettability after aging	8 ± 4°[c]	not measured	~6°[d]	110°[d]	~25°[d]	N/A	N/A	N/A	N/A	N/A	N/A
bacterial inhibition	99 ± 1%	~99%	~99%[e]	93.30%[e]	~99%[e]	71%	>99% (static), 91% (dynamic)[e]	98.8–96.9%	~97.5%	99.6–96%	~96%[e]
bacterial inhibition after aging	73 ± 13%	~99% (vertical storage)	not measured	94.8% (0.4 m s^{-1}, 10 days)[e]	not measured	N/A	N/A	N/A	N/A	N/A	N/A
field test	Y	N	N	N	N	N	Y	N	N	N	N
transparency (underwa-ter)	>80%	N/A	not measured	>93%	N/A	N/A	N/A	N/A	N/A	N/A	N/A
shapable	Y	Y[g]	N	N	N	N/A	Y[f]	Y[f]	Y[g]	N	Y[g]

[a]The most commonly employed lubricants are silicone oil and perfluoropolyethers (PFPE). [b]These two papers are related to same type of substrate. [c]Water roll-off angle. [d]Water contact angle hysteresis. [e]Calculated from reported data. [f]Not explicitly stated, but is consistent with material properties. [g]Conforms to the shape of the substrate.

ACS Appl. Mater. Interfaces 2018, 10, 4173–4182
DOI: 10.1021/acsami.7b14736

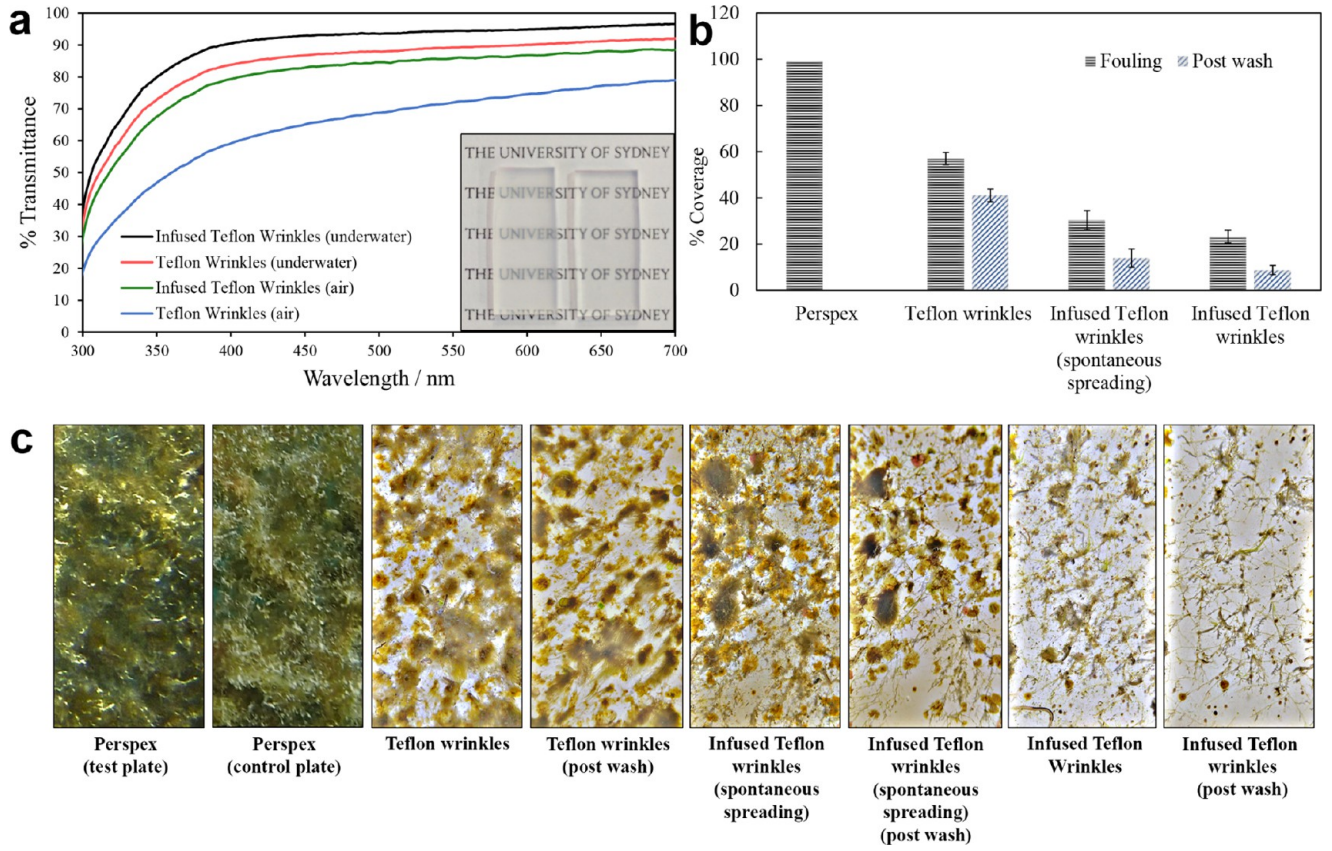

Figure 3. (a) Transmission spectra for Teflon wrinkles and infused Teflon wrinkles in both air and water. Inset: optical image showing the increased transmittance gained from infusion on the right-hand side sample; (b) average percentage coverage of fouling on surfaces tested in the ocean for 7 weeks, and after washing with water (post wash; Perspex support plate was not washed); error bars are standard error; (c) optical images of fouled surfaces, after 7 weeks of testing in the ocean, and after being washed.

portion of surface). This ability greatly increases the range of scenarios in which the surfaces can be employed.

Transparency of Infused Surfaces. Infusion of the surfaces have the additional benefit of making the surfaces more transparent when prepared using transparent substrates (polyshrink comes in a number of varieties including transparent). The wrinkled surfaces scatter incident light, reducing the transparency of the substrate. By infusing the wrinkled substrates with silicone oil, the transparency is increased from 85 to 90% throughout the visible range in water and from around 60 to 85% in air, Figure 3a. This aspect makes these surfaces ideally suited to protect underwater sensors and cameras from fouling.

Marine Fouling Test. Results from the adhesion tests of a single bacterial species may not reflect real-world scenarios: different bacterial species have different affinities to an immobilized liquid layer surface,[37] and the overall fouling of a surface cannot be predicted based on an individual bacterial species.[38] Therefore, we conduct field tests of our surfaces in a marine environment (Watsons Bay, NSW, see Materials and Methods). The site was selected due to its proximity to the open ocean, ensuring that the surfaces are exposed to a constant flow of ocean water. Support plates with the samples attached are zip-tied to a shark net below the tideline, facing north, to maximize growth by maximizing sun exposure.

Two support Perspex plates are used: on the first, referred to as "Control Plate", are glued only Teflon wrinkled surfaces (as controls). On the second plate, referred to as "Test Plate", are glued both infused Teflon wrinkles and uninfused Teflon wrinkles. On the test plate, it is predicted that the silicone oil can creep from the infused surfaces to the uninfused surfaces while underwater, so the control plate acts as the real benchmark without any silicone oil. The infused and uninfused surfaces on the test plate are interspersed to mitigate any possible spatial effects in fouling. The control plate is placed approx. 1 m from the test plate. After 7 weeks of testing, the two Perspex support plates are heavily fouled, and completely covered with algae (Figure 3c, Perspex (test plate) and Perspex (control plate)).

The plates are photographed at intermediate stages of the study to qualitatively monitor fouling, but as the images were captured *in situ* underwater, they are not of high enough quality to analyze for surface coverage (see Figures S10 and S11). The level of fouling is reported at the end of the test (7 weeks): Figure 3b shows fouling as the percentage surface coverage, and Figure 3c shows representative optical images. There is no significant difference between the level of fouling on the Teflon wrinkles and the infused Teflon wrinkles mounted on the same test plate (p = 0.17). The Teflon wrinkles adjacent to infused Teflon wrinkles appear to have been infused with silicone oil spreading from the infused surfaces (labeled "Infused Teflon wrinkles (spontaneous spreading)" in Figure 3b). This spreading even under water is entirely expected, given the ultraspreading properties of silicone oil.[39] Silicone oil completely spreads underwater on Teflon (CA = 0°, Figure 1c2), but does not form a stable film on Perspex (CA = 120°, Figure S12), which is why the support Perspex plates are entirely fouled. The close proximity of the infused Teflon wrinkles to the initially uninfused surfaces on the test plate contributes to silicone oil spreading. On the

DOI: 10.1021/acsami.7b14736
ACS Appl. Mater. Interfaces 2018, 10, 4173−4182

other hand, there is a significant difference between all of the surfaces on the test plate and those on the control plate ($p < 0.05$). Infused Teflon wrinkles have only about 23% of their surface fouled upon immersion in the ocean for 7 weeks, much lower than the Perspex support sheets (99%), lower than the uninfused Teflon wrinkles (57%), and lower than the Teflon wrinkles that are infused by spontaneous underwater spreading (30%) (Figure 3b). The difference between the test and control plates indicates that infusion with silicone oil was key in reducing fouling of the surfaces.

Our surfaces have the additional benefit of being foul-release coatings, i.e., coatings that reduce the adhesion of fouling species to the surface and make it easier to remove the fouling once it occurs.[40] Perfluorinated polymers are already used as foul-releasing materials (e.g., Intersleek 900 produced by AkzoNobel), and the length scale of the wrinkles is smaller than that of fouling species, further reducing the adhesion.[40] This suggests that our control Teflon samples already have a foul-releasing function. To test the foul-releasing properties, the fouled test and control surfaces are sprayed with water. Example results of this treatment are given in Figure 3b,c (post wash). The infused surfaces have 65% of their fouling removed upon washing, as compared to only 30% for the uninfused control surfaces, indicating that the infused silicone oil aids in foul-releasing and that an approach to antifouling using infused surfaces is better than approaches based on low surface energy and structural elements alone.

Comparison to Other SLIPS. Table 3 provides a detailed comparison with respect to bacterial fouling and oil retention between our surfaces and those in papers published in the past few years. Table 3 is not an exhaustive review in either the properties being compared or in the list of developed SLIPS, but focuses on the most relevant papers that in the past few years have addressed bacterial fouling on lubricant-infused surfaces. Integral to the performance of SLIPS is the stability of the lubricating liquid layer. The fluid dynamics of the depletion of this layer have been investigated,[10,11,30,41] but the effect of the depletion of the liquid layer on applications is rarely investigated. Our SLIPS compare well to the published results in many aspects such as bacterial adhesion and their functionality (being transparent and moldable).

As shown in Table 3, a comparison between the published results is not straightforward, as the method of aging is different and the performance is measured in different ways. There are few published studies that examine the performance of SLIPS after they have been aged, either in real-world scenarios or under simulated conditions. Even rarer is the testing of antifouling ability after aging. Simulated aging is usually through exposure to underwater shear, as this is the most likely route to the failure of surfaces in anti-biofouling applications. For example, Wang et al.[8] subjected their surfaces to 0.1−0.8 m s^{-1} flow by shaking on an orbital shaker and to ultrasonic vibration. Exposure to flow for 20 days sees the contact angle hysteresis increase to 55−110°, whereas exposure to the vibration condition sees an increase to 110° in just 1 h. Exposure to a flow of a bacterial solution (0.4 m s^{-1}) for 10 days leads to an increase in antifouling performance, compared to 10 days in static conditions. This increase is attributed to reduced bacterial adhesion due to the shear. Our surfaces retain a low roll-off angle more effectively after significant shearing, and in our case, the performance is related directly to retained oil (Table 2). Wei et al. reported a ∼50−65% reduction in oil on their surface (as measured through mass change) after centrifuging for 1 min at 3500 rpm,[9] which induced a slight increase in the contact angle hysteresis. However, Wei et al. do not test how the reduction in oil influences the biofouling of their surfaces. By comparison, our surfaces are shown to still inhibit 86% of bacterial fouling after similar oil depletion. Doll et al. tested their surfaces for biofouling ability after storing them vertically for 15 days and reported no degradation in the antifouling performance.[42] Although this is an interesting result, the ageing treatment cannot be easily compared to our more aggressive shearing.

Our laboratory results show that under simulated ocean shear, although some lubricant is clearly lost, there is only a small decrease in the slippery behavior of the surface (a result confirmed in the literature). To our knowledge, however, no group has tested bacterial attachment on a surface aged using underwater shear, which is a key aspect to moving toward their successful application. As shown in this work, resistance to fouling from a single genus of bacteria does not fully translate into real-world antifouling ability. Our surfaces show 99% reduction in marine bacterial growth, and this converts to fouling in the ocean being inhibited but not entirely prevented over 7 weeks. To our knowledge, only one other study has examined the efficacy of SLIPS in a field setting,[16] by testing the attachment of mussels and other fouling species on infused PDMS substrates. A direct comparison of our SLIPS with others with similar surface features is difficult, as only Yuan et al. have a similarly wrinkled surface.[43] Their surfaces show similar levels of bacterial inhibition and are also moldable, but not transparent.

SLIPS are inherently limited by the gradual loss of their lubricating layer, which in turn leads to the degradation in properties, such as an increase in the roll-off angle, contact angle hysteresis, or fouling. For SLIPS to be adopted for applications, their design needs to be optimized to retain oil under long-term shear. One promising approach in this direction is the inclusion of a biomimetic vascularized system to replenish the lubricating layer as it is removed.[41]

CONCLUSIONS

In conclusion, for the first time the volume of lubricant required for lubricant-infused surfaces to be slippery and antifouling was quantified using a simple fluorescence protocol that is applicable to many nonporous, nontransparent solid substrates. The knowledge of the amount of lubricant present on a surface is crucial to understand the potential and limitations of these systems in applications. Remarkably, the Teflon wrinkled surfaces retain sufficient silicone oil (0.02−0.04 μL cm^{-2}) after 2 weeks of vigorous shear in seawater to have slippery properties and to inhibit marine bacteria attachment. Infused wrinkled Teflon surfaces are much more effective than Perspex and even uninfused wrinkled Teflon surfaces at reducing algal attachment. The near complete inhibition of bacterial fouling in the laboratory does not fully translate to real-world applications due to lubricant depletion, but the algal attachment is reduced even after 7 weeks of depletion. The efficacy of antifouling surfaces should not only be tested in the laboratory, but also in real-world scenarios to ensure that their performance is not too adversely affected by the constant shear experienced in the ocean.

The minimal volume of silicone oil needed for a surface to be effective was measured, and it was shown that not all of the oil is lost even under high shear for extended periods. In turn, the volume of silicone oil lost into the environment is correspondingly minimal. This constitutes a good premise for a sustainable and benign antifouling coating. The option of high

DOI: 10.1021/acsami.7b14736
ACS Appl. Mater. Interfaces 2018, 10, 4173−4182

transparency makes these surfaces suited to protect underwater sensors and cameras from bacterial and microorganism fouling. Their high efficiency, robustness, and simple fabrication make these antifouling surfaces promising for a variety of applications.

■ ASSOCIATED CONTENT

Supporting Information

The Supporting Information is available free of charge on the ACS Publications website at DOI: 10.1021/acsami.7b14736.

Additional data including schematic of fabrication of lubricant-infused wrinkled surfaces, SEM and AFM micrographs of wrinkles, roll-off angles and wetting ridge on infused surfaces, self-healing of scratches, staining of noninfused surfaces, chemical identification of polyethylene shrinkwrap, toxicity of silicone oil (PDF)

■ AUTHOR INFORMATION

Corresponding Author

*E-mail: chiara.neto@sydney.edu.au.

ORCID

Chiara Neto: 0000-0001-6058-0885

Author Contributions

The manuscript was written through contributions of all of the authors. All of the authors have given approval to the final version of the manuscript.

Funding

The University of Sydney for co-funding Smith-Palmer's visit.

Notes

The authors declare no competing financial interest.

■ ACKNOWLEDGMENTS

The authors acknowledge The University of Sydney for co-funding Smith-Palmer's visit. The authors acknowledge A/Prof. Ross Coleman and Woollhara Municipal Council for facilitating the field tests in Watsons Bay; and the facilities and the scientific and technical assistance of the Australian Microscopy & Microanalysis Research Facility at the Australian Centre for Microscopy & Microanalysis at the University of Sydney.

■ REFERENCES

(1) Aizenberg, J. Slippery Liquid-Infused Porous Surfaces. *J. Ocean Technol.* **2014**, *9*, 113−114.

(2) Fitridge, I.; Dempster, T.; Guenther, J.; de Nys, R. The impact and control of biofouling in marine aquaculture: a review. *Biofouling* **2012**, *28*, 649−669.

(3) Banerjee, I.; Pangule, R. C.; Kane, R. S. Antifouling Coatings: Recent Developments in the Design of Surfaces That Prevent Fouling by Proteins, Bacteria, and Marine Organisms. *Adv. Mater.* **2011**, *23*, 690−718.

(4) Epstein, A. K.; Wong, T.-S.; Belisle, R. A.; Boggs, E. M.; Aizenberg, J. Liquid-infused structured surfaces with exceptional anti-biofouling performance. *Proc. Natl. Acad. Sci. U.S.A.* **2012**, *109*, 13182−13187.

(5) MacCallum, N.; Howell, C.; Kim, P.; Sun, D.; Friedlander, R.; Ranisau, J.; Ahanotu, O.; Lin, J. J.; Vena, A.; Hatton, B.; Wong, T.-S.; Aizenberg, J. Liquid-Infused Silicone As a Biofouling-Free Medical Material. *ACS Biomater. Sci. Eng.* **2015**, *1*, 43−51.

(6) Leslie, D. C.; Waterhouse, A.; Berthet, J. B.; Valentin, T. M.; Watters, A. L.; Jain, A.; Kim, P.; Hatton, B. D.; Nedder, A.; Donovan, K.; Super, E. H.; Howell, C.; Johnson, C. P.; Vu, T. L.; Bolgen, D. E.; Rifai, S.; Hansen, A. R.; Aizenberg, M.; Super, M.; Aizenberg, J.; Ingber, D. E. A bioinspired omniphobic surface coating on medical devices prevents thrombosis and biofouling. *Nat. Biotechnol.* **2014**, *32*, 1134−1140.

(7) Zhang, P.; Lin, L.; Zang, D.; Guo, X.; Liu, M. Designing Bioinspired Anti-Biofouling Surfaces based on a Superwettability Strategy. *Small* **2017**, *13*, No. 1503334.

(8) Wang, P.; Zhang, D.; Sun, S.; Li, T.; Sun, Y. Fabrication of Slippery Lubricant-Infused Porous Surface with High Underwater Transparency for the Control of Marine Biofouling. *ACS Appl. Mater. Interfaces* **2017**, *9*, 972−982.

(9) Wei, C.; Zhang, G.; Zhang, Q.; Zhan, X.; Chen, F. Silicone Oil-Infused Slippery Surfaces Based on Sol−Gel Process-Induced Nanocomposite Coatings: A Facile Approach to Highly Stable Bioinspired Surface for Biofouling Resistance. *ACS Appl. Mater. Interfaces* **2016**, *8*, 34810−34819.

(10) Wexler, J. S.; Jacobi, I.; Stone, H. A. Shear-Driven Failure of Liquid-Infused Surfaces. *Phys. Rev. Lett.* **2015**, *114*, No. 168301.

(11) Liu, Y.; Wexler, J. S.; Schonecker, C.; Stone, H. A. Effect of viscosity ratio on the shear-driven failure of liquid-infused surfaces. *Phys. Rev. Fluids* **2016**, *1*, No. 074003.

(12) Wexler, J. S.; Grosskopf, A.; Chow, M.; Fan, Y.; Jacobi, I.; Stone, H. A. Robust liquid-infused surfaces through patterned wettability. *Soft Matter* **2015**, *11*, 5023−5029.

(13) Kim, P.; Kreder, M. J.; Alvarenga, J.; Aizenberg, J. Hierarchical or Not? Effect of the Length Scale and Hierarchy of the Surface Roughness on Omniphobicity of Lubricant-Infused Substrates. *Nano Lett.* **2013**, *13*, 1793−1799.

(14) Bazyar, H.; Javadpour, S.; Lammertink, R. G. H. On the Gating Mechanism of Slippery Liquid Infused Porous Membranes. *Adv. Mater. Interfaces* **2016**, *3*, No. 1600025.

(15) Daniel, D.; Timonen, J. V. I.; Li, R.; Velling, S. J.; Aizenberg, J. Oleoplaning droplets on lubricated surfaces. *Nat. Phys.* **2017**, *13*, 1020−1025.

(16) Amini, S.; Kolle, S.; Petrone, L.; Ahanotu, O.; Sunny, S.; Sutanto, C. N.; Hoon, S.; Cohen, L.; Weaver, J. C.; Aizenberg, J.; Vogel, N.; Miserez, A. Preventing mussel adhesion using lubricant-infused materials. *Science* **2017**, *357*, 668−673.

(17) Anand, S.; Paxson, A. T.; Dhiman, R.; Smith, J. D.; Varanasi, K. K. Enhanced Condensation on Lubricant-Impregnated Nanotextured Surfaces. *ACS Nano* **2012**, *6*, 10122−10129.

(18) Wong, T.-S.; Kang, S. H.; Tang, S. K. Y.; Smythe, E. J.; Hatton, B. D.; Grinthal, A.; Aizenberg, J. Bioinspired self-repairing slippery surfaces with pressure-stable omniphobicity. *Nature* **2011**, *477*, 443−447.

(19) Lafuma, A.; Quéré, D. Slippery pre-suffused surfaces. *Europhys. Lett.* **2011**, *96*, No. 56001.

(20) Kim, P.; Wong, T.-S.; Alvarenga, J.; Kreder, M. J.; Adorno-Martinez, W. E.; Aizenberg, J. Liquid-Infused Nanostructured Surfaces with Extreme Anti-Ice and Anti-Frost Performance. *ACS Nano* **2012**, *6*, 6569−6577.

(21) Ma, W.; Higaki, Y.; Otsuka, H.; Takahara, A. Perfluoropolyether-infused nano-texture: a versatile approach to omniphobic coatings with low hysteresis and high transparency. *Chem. Commun.* **2013**, *49*, 597−599.

(22) Scarratt, L. R. J.; Hoatson, B. S.; Wood, E. S.; Hawkett, B. S.; Neto, C. Durable Superhydrophobic Surfaces via Spontaneous Wrinkling of Teflon. *ACS Appl. Mater. Interfaces* **2016**, *8*, 6743−6750.

(23) Wei, Q.; Schlaich, C.; Prévost, S.; Schulz, A.; Böttcher, C.; Gradzielski, M.; Qi, Z.; Haag, R.; Schalley, C. A. Supramolecular Polymers as Surface Coatings: Rapid Fabrication of Healable Superhydrophobic and Slippery Surfaces. *Adv. Mater.* **2014**, *26*, 7358−7364.

(24) Manna, U.; Lynn, D. M. Fabrication of Liquid-Infused Surfaces Using Reactive Polymer Multilayers: Principles for Manipulating the Behaviors and Mobilities of Aqueous Fluids on Slippery Liquid Interfaces. *Adv. Mater.* **2015**, *27*, 3007−3012.

(25) Bico, J.; Thiele, U.; Quéré, D. Wetting of textured surfaces. *Colloids Surf., A* **2002**, *206*, 41−46.

(26) Smith-Palmer, T.; Lin, S.; Oguejiofor, I.; Leng, T.; Pustam, A.; Yang, J.; Graham, L. L.; Wyeth, R. C.; Bishop, C. D.; DeMont, M. E.;

Pink, D. In Situ Confocal Raman Microscopy of Hydrated Early Stages of Bacterial Biofilm Formation on Various Surfaces in a Flow Cell. *Appl. Spectrosc.* **2015**, *70*, 289−301.
(27) Quéré, D. Wetting and Roughness. *Annu. Rev. Mater. Res.* **2008**, *38*, 71−99.
(28) Smith, J. D.; Dhiman, R.; Anand, S.; Reza-Garduno, E.; Cohen, R. E.; McKinley, G. H.; Varanasi, K. K. Droplet mobility on lubricant-impregnated surfaces. *Soft Matter* **2013**, *9*, 1772−1780.
(29) Cassie, A. B. D.; Baxter, S. Wettability of porous surfaces. *Trans. Faraday Soc.* **1944**, *40*, 546−551.
(30) Kim, J.-H.; Rothstein, J. P. Delayed lubricant depletion on liquid-infused randomly rough surfaces. *Exp. Fluids* **2016**, *57*, No. 81.
(31) In all cases, silicone oil (o) is likely to cloak a water droplet (w) in air (a), as the spreading parameter $S_{ow(a)} = \gamma_{wa} - \gamma_{wo} - \gamma_{oa} = 72 - 44 - 18.4 = 9.6$ mN m^{-1} is positive.
(32) Scarratt, L. R. J.; Steiner, U.; Neto, C. A Review on the Mechanical and Thermodynamic Robustness of Superhydrophobic Surfaces. *Adv. Colloid Interface Sci.* **2017**, *246*, 133−152.
(33) Yoon, J.-Y.; Garrell, R. L. *Biomolecular Adsorption in Microfluidics*, 2nd ed.; New York, NY; Springer, 2015.
(34) Lichter, J. A.; Thompson, M. T.; Delgadillo, M.; Nishikawa, T.; Rubner, M. F.; Van Vliet, K. J. Substrata Mechanical Stiffness Can Regulate Adhesion of Viable Bacteria. *Biomacromolecules* **2008**, *9*, 1571−1578.
(35) Kolewe, K. W.; Peyton, S. R.; Schiffman, J. D. Fewer Bacteria Adhere to Softer Hydrogels. *ACS Appl. Mater. Interfaces* **2015**, *7*, 19562−19569.
(36) Vogel, N.; Belisle, R. A.; Hatton, B.; Wong, T.-S.; Aizenberg, J. Transparency and damage tolerance of patternable omniphobic lubricated surfaces based on inverse colloidal monolayers. *Nat. Commun.* **2013**, *4*, No. 2176.
(37) Kovalenko, Y.; Sotiri, I.; Timonen, J. V. I.; Overton, J. C.; Holmes, G.; Aizenberg, J.; Howell, C. Bacterial Interactions with Immobilized Liquid Layers. *Adv. Healthcare Mater.* **2017**, *6*, No. 1600948.
(38) Bernbom, N.; Ng, Y. Y.; Olsen, S. M.; Gram, L. Pseudoalteromonas spp. Serve as Initial Bacterial Attractants in Mesocosms of Coastal Waters but Have Subsequent Antifouling Capacity in Mesocosms and when Embedded in Paint. *Appl. Environ. Microbiol.* **2013**, *79*, 6885−6893.
(39) Tanner, L. H. The spreading of silicone oil drops on horizontal surfaces. *J. Phys. D: Appl. Phys.* **1979**, *12*, 1473−1485.
(40) Lejars, M.; Margaillan, A.; Bressy, C. Fouling Release Coatings: A Nontoxic Alternative to Biocidal Antifouling Coatings. *Chem. Rev.* **2012**, *112*, 4347−4390.
(41) Howell, C.; Vu, T. L.; Lin, J. J.; Kolle, S.; Juthani, N.; Watson, E.; Weaver, J. C.; Alvarenga, J.; Aizenberg, J. Self-Replenishing Vascularized Fouling-Release Surfaces. *ACS Appl. Mater. Interfaces* **2014**, *6*, 13299−13307.
(42) Doll, K.; Fadeeva, E.; Schaeske, J.; Ehmke, T.; Winkel, A.; Heisterkamp, A.; Chichkov, B. N.; Stiesch, M.; Stumpp, N. S. Development of Laser-Structured Liquid-Infused Titanium with Strong Biofilm-Repellent Properties. *ACS Appl. Mater. Interfaces* **2017**, *9*, 9359−9368.
(43) Yuan, S.; Luan, S.; Yan, S.; Shi, H.; Yin, J. Facile Fabrication of Lubricant-Infused Wrinkling Surface for Preventing Thrombus Formation and Infection. *ACS Appl. Mater. Interfaces* **2015**, *7*, 19466−19473.
(44) Xiao, L.; Li, J.; Mieszkin, S.; Di Fino, A.; Clare, A. S.; Callow, M. E.; Callow, J. A.; Grunze, M.; Rosenhahn, A.; Levkin, P. A. Slippery Liquid-Infused Porous Surfaces Showing Marine Antibiofouling Properties. *ACS Appl. Mater. Interfaces* **2013**, *5*, 10074−10080.
(45) Zhang, P.; Chen, H.; Zhang, L.; Zhang, D. Anti-adhesion effects of liquid-infused textured surfaces on high-temperature stainless steel for soft tissue. *Appl. Surf. Sci.* **2016**, *385*, 249−256.
(46) Yuan, S.; Li, Z.; Song, L.; Shi, H.; Luan, S.; Yin, J. Liquid-Infused Poly(styrene-b-isobutylene-b-styrene) Microfiber Coating Prevents Bacterial Attachment and Thrombosis. *ACS Appl. Mater. Interfaces* **2016**, *8*, 21214−21220.
(47) Tesler, A. B.; Kim, P.; Kolle, S.; Howell, C.; Ahanotu, O.; Aizenberg, J. Extremely durable biofouling-resistant metallic surfaces based on electrodeposited nanoporous tungstite films on steel. *Nat. Commun.* **2015**, *6*, No. 8649.

DOI: 10.1021/acsami.7b14736
ACS Appl. Mater. Interfaces 2018, 10, 4173−4182